

Like host, like parasite: intraspecific divergence in a polystomatid flatworm parasite across South Africa echoes that of its frog host

Non Peer-reviewed author version

Schoeman, Anneke Lincoln; KMENTOVA, Nikol; VANHOVE, Maarten & Du Preez, Louis Heyns (2022) Like host, like parasite: intraspecific divergence in a polystomatid flatworm parasite across South Africa echoes that of its frog host.

DOI: 10.1101/2022.03.15.483565

Handle: <http://hdl.handle.net/1942/37126>

1 Like host, like parasite: intraspecific divergence in a 2 polystomatid flatworm parasite across South Africa 3 echoes that of its frog host

**4 Anneke Lincoln SCHOEMAN^{1,2,3}, Nikol KMENTOVÁ^{4,5}, Maarten PM VANHOVE^{4,5}, and
5 Louis Heyns DU PREEZ^{1,3}**

**6 ¹African Amphibian Conservation Research Group, Unit for Environmental Sciences and Management,
7 North-West University, Potchefstroom Campus, 11 Hoffman Street, Potchefstroom 2531, South Africa**

8 ²DSI-NRF Centre of Excellence for Invasion Biology, Stellenbosch, South Africa

9 ³South African Institute for Aquatic Biodiversity, Private Bag 1015, Grahamstown 6140, South Africa

**10 ⁴Department of Botany and Zoology, Faculty of Science, Masaryk University, Kotlářská 2, 611 37 Brno,
11 Czech Republic**

**12 ⁵Hasselt University, Centre for Environmental Sciences, Research Group Zoology: Biodiversity &
13 Toxicology, Agoralaan Gebouw D, B-3590 Diepenbeek, Belgium**

14 Correspondence Anneke Lincoln Schoeman; email: anneke.lincoln@gmail.com

15 ABSTRACT

16 The African Clawed Frog *Xenopus laevis*, a global invader, exhibits marked phylogeographic divergence
17 among native populations in southern Africa, which enhances its invasive potential. The polystomatid
18 flatworm *Protopolystoma xenopodis*, as the frog's most frequently co-introduced metazoan parasite,
19 may be the ideal biological tag for the frog's movement, if corresponding divergence can be demon-
20 strated. In an integrative approach, we utilised morphometrics and molecular markers to assess
21 divergence in *P. xenopodis* in its native range. We measured twelve key morphological characters
22 from 23 flatworms and compared these statistically between flatworms collected to the north and
23 south of the Great Escarpment Mountain Range in South Africa. Phylogenetic analyses were based
24 on three concatenated markers, namely *28S* and *12S rDNA* and *COX1*, from six flatworms. The
34 combination of five morphological characters, which involve egg size, gut morphology and size of the
25 attachment hooks, differentiated northern and southern populations of *P. xenopodis* in South Africa.
26 The multilocus phylogenetic analyses supported these findings, showing a well-supported cluster
27 of northern *P. xenopodis*. These findings suggest that taxonomic studies of polystomatid flatworms
28 should make use of geographically representative data sets that consider both morphological and
29 molecular evidence. Moreover, the findings demonstrate that the frog host and flatworm parasite exhibit
30 corresponding phylogeographic structuring in the native range. Consequently, the phylogeography of
31 *P. xenopodis*, both in the native and invasive range of its host, may act as a key piece of evidence to
32 reconstruct past invasion pathways of *X. laevis*.

35 Keywords: integrative taxonomy; phylogeography; *Protopolystoma xenopodis*; *Xenopus*
37
36 *laevis*

38 1 INTRODUCTION

39 Variability, which promotes the adaptability and viability of populations in changing environments,
40 is a factor to be reckoned with when it comes to the invasion success of alien species, as
41 has been shown for several taxonomic groups in aquatic ecosystems (Wellband *et al.*, 2017).
42 Consequently, a thorough understanding of the evolutionary history of an invasive species in its
43 native range is essential to assess its potential to colonise and adapt to novel surroundings

44 (Lee & Gelembiuk, 2008). This is equally true for the co-introduced parasites of free-living
45 invasive species, which make out most non-native species (Torchin *et al.*, 2003). Yet, alien
46 parasites are often overlooked in the study of biological invasions (Blackburn & Ewen, 2017).

47 Worldwide, the African Clawed Frog *Xenopus laevis* (Daudin 1802) (Anura: Pipidae) is
48 one of the most widespread amphibians. Its native range covers much of sub-Saharan Africa
49 (Furman *et al.*, 2015). Invasive populations of this frog can be found in Asia, Europe and North
50 and South America (Measey *et al.*, 2012). Wherever *X. laevis* occurs, it harbours a diverse
51 and unique parasite fauna (Tinsley, 1996). One of *X. laevis*' most prevalent parasites is the
52 host-specific flatworm *Protopolystoma xenopodis* (Price, 1943) (Monogenea: Polystomatidae),
53 a sanguivorous inhabitant of the frog's bladder in its adult form. In the native range of southern
54 Africa, *P. xenopodis* is a common feature of *X. laevis* parasite assemblages, where it has been
55 recovered from more than 90% of *X. laevis* populations and more than 50% of all sampled hosts
56 in a recent survey (Schoeman *et al.*, 2019). Moreover, in the context of the global invasive status
57 of *X. laevis*, *P. xenopodis* emerges as its most frequently co-introduced metazoan parasite and
58 has been reported from hosts in France, Portugal, the United Kingdom and the United States
59 (Tinsley & Jackson, 1998b; Kuperman *et al.*, 2004; Rodrigues, 2014; Schoeman *et al.*, 2019).

60 In general, *P. xenopodis* is differentiated from its congeners, which infect other *Xenopus*
61 species in Africa, based upon the morphology of the gut, large posterior attachment hooks and
62 spines on the male reproductive organs (Tinsley & Jackson, 1998b). The gut of *Protopolystoma*
63 spec. bifurcates after the pharynx into two caeca, which branch out even further into diverticula
64 that may fuse to form post-ovarian inter-caecal anastomoses (Tinsley & Jackson, 1998b). The
65 number of diverticula and anastomoses varies within and between species (Tinsley & Jackson,
66 1998b). All *Protopolystoma* spec. possess a pair of large hooks, or hamuli, with two roots
67 and a sharpened terminal hook, used to attach to the wall of the host's bladder (Tinsley &
68 Jackson, 1998b). Due to their size, complex shape and sclerotisation, the morphology of
69 the large hamuli is the most taxonomically informative feature among members of the genus

70 (Tinsley & Jackson, 1998b). Finally, *Protopolystoma* spec. have a muscular, bulb-shaped male
71 reproductive organ armed with sixteen spines that are arranged in two concentric rings of
72 eight spines each (Tinsley & Jackson, 1998b). It is hard to obtain reliable measurements of
73 these spines but *P. xenopodis* appears to have much shorter spines than its congeners (Tinsley
74 & Jackson, 1998b). In their redescription of *P. xenopodis*, Tinsley & Jackson (1998b) noted
75 geographical variation in the size of the genital spines between southern and more northerly
76 populations across sub-Saharan Africa. The authors also noted marked intraspecific variation in
77 the morphology of the large hamulus and the caecal branches, although this was not correlated
78 with geographic distance (Tinsley & Jackson, 1998b).

79 Given the wide distribution of this parasite across the globe, possible cryptic diversity,
80 explored through both morphological and molecular data, is worth investigating as an essential
81 building block of bio-invasion research (Mazzamuto *et al.*, 2016). In addition to illuminating the
82 evolutionary potential of this alien parasite, the exploration of the intraspecific divergence in
83 *P. xenopodis* is worthwhile in the light of the phylogeographic structuring of its host *X. laevis*
84 in its native range (de Busschere *et al.*, 2016; Furman *et al.*, 2015). Previous studies on the
85 morphology and genetics of *X. laevis* have identified marked divergence among populations
86 in southern Africa (Grohovaz *et al.*, 1996; Measey & Channing, 2003; du Preez *et al.*, 2009;
87 Furman *et al.*, 2015; de Busschere *et al.*, 2016).

88 The intimate association between frog host and flatworm parasite would lead us to expect
89 corresponding morphological and phylogenetic divergence among the populations of *P. xeno-*
90 *podis* across southern Africa. Congruence in host-parasite phylogeographies arises as a result
91 of high host-specificity and direct life cycles, in combination with limited host-independent
92 dispersal capacity (Nieberding & Olivieri, 2007). What is more, since parasites exhibit shorter
93 generation times and greater abundance than their hosts, their phylogeographic divergence
94 is often more pronounced (Nieberding & Olivieri, 2007). Consequently, parasites can act as
95 biological magnifying glasses to further explore the host's phylogeographic structuring and

96 movement in both its native and invasive ranges (Nieberding *et al.*, 2004). For example, the
97 intraspecific morphological variation of monogenean flatworm parasites provided information on
98 the invasion history of fish in Africa and Europe (Kmentová *et al.*, 2019; Ondračková *et al.*, 2012).
99 In this framework, widespread co-introduced parasites of invasive hosts, such as *P. xenopodis*,
100 could be ideal tags to trace the translocation of host lineages—if it can be demonstrated that
101 they diverge according to a similar pattern as their hosts.

102 Therefore, the present study offers an exploratory investigation of the morphological differ-
103 ences and phylogenetic divergence in *P. xenopodis* collected from *X. laevis* from the northern-
104 most or southernmost northernmost and southernmost localities in South Africa, linked to two
105 distinct phylogeographic lineages according to de Busschere *et al.* (2016). In an integrative
106 approach, we will rely on a combination of evidence from one nuclear and two mitochon-
107 drial genes and twelve key morphological characters to assess differentiation in *P. xenopodis*
108 between the two regions. We expect (1) marked intraspecific variability in *P. xenopodis* in
109 South Africa, (2) with significant divergence between northern and southern parasites in some
110 taxonomically important morphological characters, such as gut morphology and dimensions
111 of the sclerites, and in the three molecular markers, *COX1* and *12S rDNA* and *28S rDNA*, (3)
112 which corresponds to the divergence of the host *X. laevis*.

113 2 METHODS

114 2.1 Specimen collection

115 From March to July 2017, 20 adult *X. laevis* were captured in funnel traps baited with chicken
116 liver at eight field sites across South Africa (Table 1). These sites were located near previously
117 sampled localities where the local *X. laevis* populations were genetically identified as belonging
118 to either one of two phylogeographic lineages of this frog by de Busschere *et al.* (2016), namely
119 SA1 to the southwest and SA5 to the northeast of southern Africa (Figure 1). These two
120 groups of sites lie on either side the Great Escarpment, the edge of an inland plateau that runs

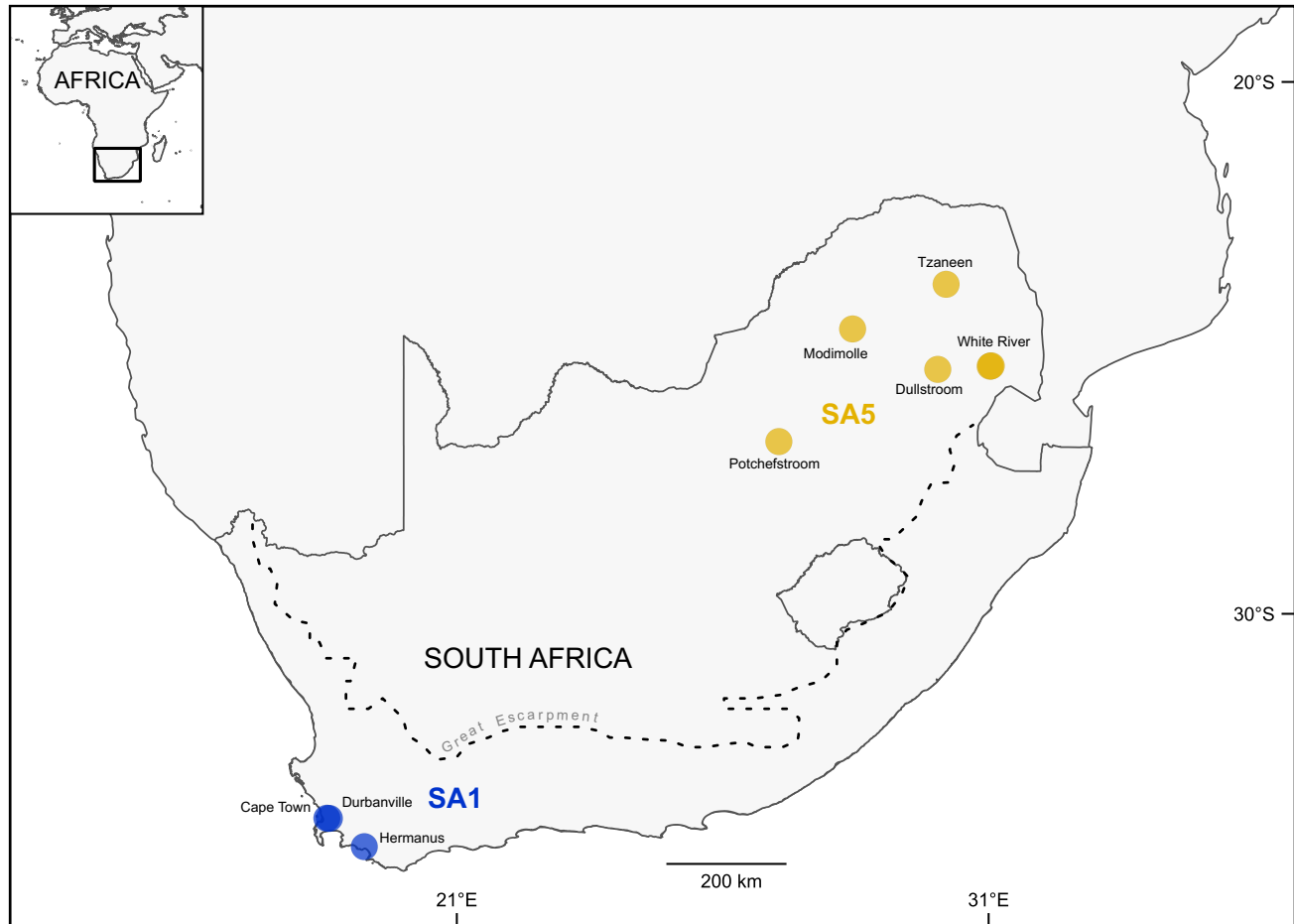


FIGURE 1 The eight localities where *Protopolystoma xenopodis* was obtained from *Xenopus laevis*, coloured according to the frogs' expected phylogeographic lineage according to de Busschere *et al.* (2016), namely SA1 (in blue) to the southwest of the Great Escarpment Mountain Range (dotted line) or SA5 (in yellow) to the northeast. The locality names, derived from the nearest town, are indicated. The map was constructed in QGIS version 3.10.2-A Coruña (QGIS Development Team, 2018) with the Mercator projection.

121 continuously along the southwestern seaboard of southern Africa, which has been suggested
122 as a natural barrier to gene flow for *X. laevis* (Furman *et al.*, 2015). Based upon previous
123 phylogeographic work, we can expect distinct lineages of this frog to the southwest, a winter
124 rainfall region, and the northeast, a summer rainfall region, of the Escarpment (Furman *et al.*,
125 2015).

126 The frogs underwent double euthanasia according to institutional ethics guidelines under
127 ethics approval number NWU-00380-16-A5-01: first anaesthesia in 6% ethyl-3-aminobenzoate
128 methansulfonate (MS222) (Sigma-Aldrich Co., USA) and then euthanasia through pithing.

TABLE 1 Information on the geographic origin of *Xenopus laevis* and their associated *Protopolystoma xenopodis* specimens. Localities are assigned according to the expected phylogeographic lineage of *X. laevis* in South Africa (de Busschere *et al.*, 2016). Locality names refer to the nearest town and are given along with the collection date, geographic coordinates of the sampled water bodies, number of adult *X. laevis* hosts captured (N_X) and number of *P. xenopodis* parasites collected for morphometry ($N_{P[m]}$) and DNA sequencing ($N_{P[s]}$).

Locality	Date	Coordinates	N_X	$N_{P[m]}$	$N_{P[s]}$
SA1 host lineage (southwestern South Africa)					
Cape Town, Western Cape	June 2017	33.8355 °S; 18.5528 °E	2	2	1
Durbanville, Western Cape	July 2017	33.8392 °S; 18.6003 °E	2	4	0
Hermanus, Western Cape	June 2017	34.3702 °S; 19.2571 °E	3	4	1
SA5 host lineage (northeastern South Africa)					
Dullstroom, Mpumalanga Province	April 2017	25.3981 °S; 30.0380 °E	4	3	1
Modimolle, Limpopo Province	April 2017	24.6384 °S; 28.4369 °E	2	2	1
Potchefstroom, North-West Province	March 2017	26.7555 °S; 27.0506 °E	3	3	1
Tzaneen, Limpopo Province	May 2017	23.7988 °S; 30.1951 °E	2	2	1
White River, Mpumalanga Province	April 2017	25.3391 °S; 31.0226 °E	1	1	0
		25.3320 °S; 31.0433 °E	2	2	0

129 Frogs were dissected and adult specimens of *P. xenopodis* were obtained from the excretory
 130 bladder. The 29 retrieved polystomatids were processed for either morphological or molecular
 131 analyses (Table 1).

132 2.2 Morphometrical analyses

133 In total, 23 of the retrieved polystomatids from the eight localities were processed for morpho-
 134 logical analyses. The live polystomatids were placed in a drop of tap water on a microscope
 135 slide and gently heated from underneath until they relaxed, following Snyder & Clopton (2005).
 136 They were then fixed in 10% neutral buffered formalin or 70% ethanol under coverslip pressure.
 137 Polystomatids preserved in both 10% neutral buffered formalin and 70% ethanol were hydrated
 138 through a decreasing ethanol series to tap water, with 10 minutes spent on each step. The
 139 specimens were stained overnight in acetocarmine. Thereafter, the specimens were dehy-
 140 drated in an increasing ethanol series to absolute ethanol, 10 minutes per step, with colour
 141 corrections by hydrochloric acid incorporated whilst the specimens were in the 70% ethanol.
 142 The specimens were cleared in xylene and mounted in Canada balsam (Sigma-Aldrich Co.,
 143 Steinheim, Germany). The mounts were dried at 50 °C for approximately 48 hours.

144 Measurements and photomicrographs were taken on a Nikon ECLIPSE E800 compound
145 microscope in conjunction with the software NIS-Elements Documentation *version 3.22.09*
146 (Nikon Instruments Inc., Tokyo, Japan). The following nine characters were measured: body
147 length from the tip of the haptor to tip of the false oral sucker, body width at the widest point,
148 length and width of the haptor, length of the ventral roots of the two large hamuli, length of the
149 dorsal roots of the two large hamuli, length of the terminal hooks of the two large hamuli and the
150 length and width of the egg (if present) at the longest and widest points, respectively (Figure 2).
151 The following three structures were counted: number of post-ovarian inter-caecal anastomoses,
152 number of medial diverticula of the caecum and number of lateral diverticula (Figure 2). The
153 hamuli and the medial and lateral diverticula from the two sides of the polystomatids were
154 measured or counted separately and then averaged for each specimen to give a single value
155 for each character for subsequent analyses.

156 The 12 characters were compared statistically based upon geographic origin (SA1 or SA5) in
157 the software R *version 4.1.2* (R Core Team, 2021). Unless otherwise mentioned, data carpentry
158 and visualisation were performed with the help of the R packages *broom* (Robinson *et al.*, 2022),
159 *factoextra* (Kassambara & Mundt, 2020), *ggdist* (Kay, 2021), *ggtext* (Wilke, 2020), *patchwork*
160 (Lin Pedersen, 2020), *png* (Urbanek, 2013), *skimr* (Waring *et al.*, 2021) and *tidyverse* (Wickham
161 *et al.*, 2019). Missing data points were imputed by the random forest method in the R package
162 *missForest* (Stekhoven, 2013) using a random seed of 666 as starting point. This method was
163 preferred since it has a non-parametric approach suitable to the small sample size and because
164 it can handle mixed variable types (Stekhoven & Bühlmann, 2012). Since certain characters
165 can vary with parasite age, or its proxy, body size, the median body length and width and haptor
166 length and width were compared between the two groups with the non-parametric Wilcoxon-
167 Mann-Whitney (WMW) test to ensure that the groups contained polystomatids of similar size
168 distributions. The WMW test was further employed to test whether there was a significant
169 difference in the median number of post-ovarian inter-caecal anastomoses and lateral and

Intraspecific divergence in *Protopolystoma xenopodis*

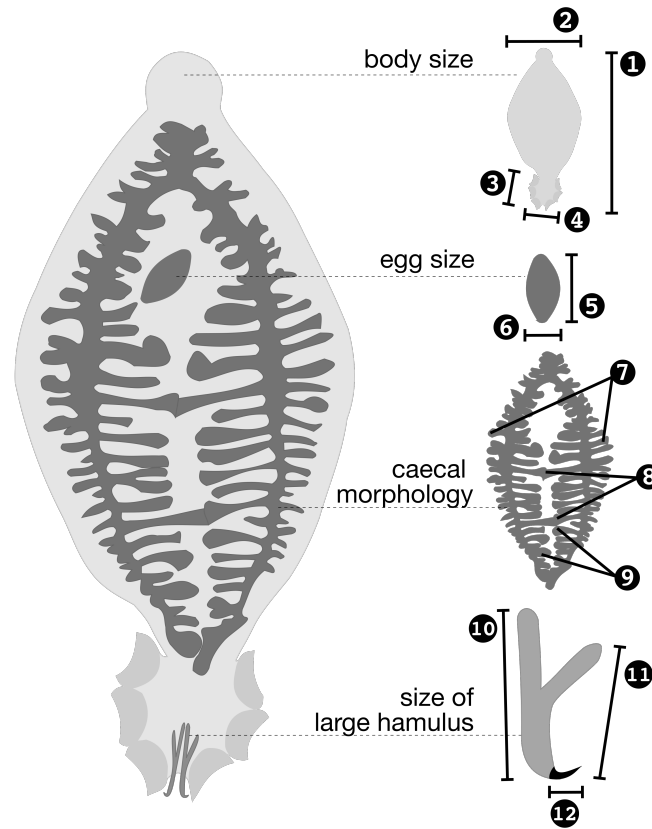


FIGURE 2 Measured morphological characters of adult *Protopolystoma xenopodis*: (1) body length, (2) body width, (3) haptor length, (4) haptor width, (5) egg length, (6) egg width, (7) number of lateral diverticula, (8) number of post-ovarian inter-caecal anastomoses, (9) number of medial diverticula, (10) length of the dorsal root of the large hamulus, (11) length of the ventral root of the large hamulus, (12) length of the terminal hook of the large hamulus.

170 medial diverticula, the median length of the terminal hook and dorsal and ventral roots of the
171 large hamuli and egg length and width between *P. xenopodis* from the two phylogeographic
172 lineages of the host. The WMW tests were performed and visualised via the R package *ggsignif*
173 (Constantin & Patil, 2021).

174 A principal components analysis (PCA), which is commonly employed in numerical taxonomy,
175 also that of monogeneans (e.g. Hahn *et al.*, 2011), was employed to evaluate the correlation
176 among polystomatids from different localities based upon the variance in the characters
177 that were shown to be significantly different between the two groups. The PCA visualised
178 whether the combination of significantly different morphological characters could discriminate
179 between polystomatids from SA1 and SA5 hosts, despite overlap in the measurements of all

180 these characters between the two groups, without taking into account geographical origin *a*
181 *priori*. The visualisation further identified the characters that contributed most to the variation
182 between groups. Since the Euclidean distances utilised in a PCA are sensitive to different
183 units of measurement, the data were column-standardised beforehand in the R package *vegan*
184 (Oksanen *et al.*, 2020) as recommended by Thorpe (1981). The PCA itself was performed in
185 base R, utilising the singular value decomposition method.

186 **2.3 Molecular and phylogenetic analyses**

187 One nuclear marker, namely *28S rDNA*, and two mitochondrial markers, namely *12S rDNA* and
188 *COX1*, were chosen for the phylogenetic analyses. These markers have been used previously
189 for both taxonomic and phylogenetic studies of Polystomatidae, leading to the availability of
190 family-specific primers for these genes (Héritier *et al.*, 2015, 2018; Verneau *et al.*, 2009).

191 Extracts of DNA were obtained from six additional polystomatid specimens from six of
192 the eight localities (Table 1) with the PCR BIO Rapid Extract PCR Kit (PCR Biosystems Ltd.,
193 London, United Kingdom). Subsequent amplification reactions were performed with 2 to
194 5 μ L extracted DNA, 1.25 μ L [0.2 μ M] forward primer and 1.25 μ L [0.2 μ M] reverse primer,
195 12.5 μ L [1 \times] master mix from the PCR BIO HS Taq Mix Red (PCR Biosystems Ltd., London,
196 United Kingdom) and PCR grade water to the final volume of 25 μ L. The nuclear *28S rDNA*
197 of the six specimens of *P. xenopodis* was amplified using the method of Verneau *et al.* (2009)
198 with the primer pair 'LSU5' (5'-TAGGTCGACCCGCTGAAAYTTAAGCA-3') (Littlewood *et al.*,
199 1997) and 'LSU1500R' (5'-GCTATCCTGAGGGAAACTTCG-3') (Tkach *et al.*, 1999). For the
200 amplification of the partial mitochondrial *12S rDNA*, the thermocycling profile, forward primer
201 '12SpolF1' (5'-YVGTGMCAGCMRYCGCGGYA-3') and one of two reverse primers, '12SpolR1'
202 (5'-TACCRTGTTACGACTTRHCTC-3') or '12SpolR9' (5'-TCGAAGATGACGGGCGATGTG-3'),
203 of Héritier *et al.* (2015) were used. Amplicons of the partial mitochondrial *COX1* gene were
204 obtained with the forward primer 'L-CO1p' (5'-TTTTTTGGGCATCCTGAGGTTTAT-3') and one
205 of two reverse primers, 'H-Cox1p2' (5'-TAAAGAAAGAACATAATGAAAATG-3') or 'H-Cox1R'

206 (5'-AACAAACAACCAAGAATCATG-3'), also using the profile of H eritier *et al.* (2015).

207 For purification and sequencing, all PCR products were sent to a commercial company
208 (Inqaba Biotec, Pretoria, South Africa) that used the ExoSAP protocol (New England Biolabs
209 Ltd., United States) for purification and obtained the sequences with BigDye[®] Terminator *version*
210 3.1 Cycle Sequencing, utilising the corresponding primer pairs used in the PCR reaction, on an
211 ABI3500XL analyser. Sequences were assembled and manually edited in Geneious *version*
212 9.0 (Saint Joseph, Missouri, United States). Sequences were uploaded to GenBank (accession
213 numbers to be added after manuscript acceptance).

214 The sequences from the six *P. xenopodis* specimens were aligned separately for each gene
215 in Seaview *version* 4.7 (Gouy *et al.*, 2010) with the MUSCLE algorithm *version* 3 at default
216 settings (Edgar, 2004). For the protein-coding *COX1*, alignment was performed on the amino
217 acid sequences, translated by the echinoderm and flatworm mitochondrial genetic code. The
218 percentage of differing bases between the sequence pairs in each alignment was calculated
219 in Geneious. Model-corrected pairwise genetic distances were calculated through maximum
220 likelihood (ML) analysis in IQ-TREE *version* 2.1.2 (Minh *et al.*, 2020), which first selected the
221 optimal model of molecular evolution for each gene with the ModelFinder selection routine
222 (Kalyaanamoorthy *et al.*, 2017) with the FreeRate heterogeneity model (Soubrier *et al.*, 2012)
223 based on the Bayesian Information Criterion (BIC). The substitution models were TPM2u + F
224 (Kimura, 1981; Soubrier *et al.*, 2012) for the partial *28S rDNA*, HKY + F + I (Gu *et al.*, 1995;
225 Posada, 2003; Soubrier *et al.*, 2012) for the partial *12S rDNA* and TIM2 + F + G (Posada, 2003;
226 Soubrier *et al.*, 2012; Yang, 1994) for the partial *COX1* gene. The same analyses calculated
227 the number of invariant and parsimony informative sites for each sequence alignment.

228 For the subsequent phylogenetic analyses, previously published *COX1*, *28S* and *12S*
229 sequences of the closely related *P. occidentalis* (accession numbers KR856179.1, KR856121.1
230 and KR856160.1, respectively) were included as outgroup (H eritier *et al.*, 2015) and the
231 sequence sets were realigned as detailed above. The aligned sequences were concatenated

232 in SequenceMatrix *version* 1.8 (Vaidya *et al.*, 2011). The optimal models of molecular evolution
233 for the *12S* and *28S rDNA* genes and the three *COX1* codon positions (Chernomor *et al.*, 2016)
234 were selected based on the BIC with the ModelFinder selection routine (Kalyaanamoorthy *et al.*,
235 2017) implemented in W-IQ-TREE *version* 1.6.7 (Trifinopoulos *et al.*, 2016). The five partitions
236 were initially analysed separately (Chernomor *et al.*, 2016) and then sequentially merged with
237 the implementation of a greedy strategy until model fit no longer improved (Kalyaanamoorthy
238 *et al.*, 2017). The new selection procedure was implemented which included the FreeRate
239 heterogeneity model (Soubrier *et al.*, 2012). The selection routine identified three partitions
240 in the alignment, namely the *12S rDNA* and *COX1* first codon position with best-fit model the
241 HKY + G (Hasegawa *et al.*, 1985; Yang, 1994), the *28S rDNA* and *COX1* second codon position
242 with TIM2 + I (Gu *et al.*, 1995; Posada, 2003) and the *COX1* third codon position with TIM2
243 (Posada, 2003).

244 For tree reconstruction, both ML analysis and Bayesian inference of phylogeny (BI) were
245 performed to increase confidence in the resulting topology. The ML tree was inferred under
246 the three partitions suggested by the selection routine. The parameter estimates were edge-
247 unlinked for all partitions. The analysis was performed in IQ-TREE *version* 1.6.7 (Nguyen
248 *et al.*, 2015), with the assessment of branch support through ultrafast bootstrapping (UFboot2;
249 Hoang *et al.*, 2018) and the Shimodaira-Hasegawa-like (SH-like) approximate likelihood ratio
250 test (SH-aLRT; Guindon *et al.*, 2010), each with 10 000 replicates.

251 The BI was performed in MrBayes *version* 3.2.6 (Ronquist *et al.*, 2012) implemented through
252 the CIPRES Science Gateway *version* 3.3 on XSEDE (Miller *et al.*, 2010). Posterior probabilities
253 were calculated with four different Metropolis-coupled Markov chains over 10^6 generations,
254 with sampling of the Markov chain every 10^3 generations. The first quarter of the samples was
255 discarded as burn-in. Stationarity of the Markov chains was reached, as indicated by a deviation
256 of split frequencies of 0.001, by a potential scale reduction factor converging to 1 and by the
257 absence of a trend in the plot of log-probabilities as function of generations. The substitution

258 models implemented in MrBayes were adapted from the selection of ModelFinder as the next
259 more complex model under the BIC in terms of substitution rates available in MrBayes. Thus,
260 the HKY model (Hasegawa *et al.*, 1985) was implemented for the first partition, allowing for a
261 discrete gamma model and the GTR (Tavaré, 1986) model was implemented with and without
262 a proportion of invariant sites for the second and third partitions, respectively. All parameter
263 estimates were edge-unlinked.

264 3 RESULTS

265 3.1 Morphological divergence

266 None of the four indicators of body size, namely body length and width and haptor length
267 and width, were significantly different between the polystomatids from the northeastern (SA5,
268 $n = 13$) and southwestern (SA1, $n = 10$) frog hosts (Figure 3*a–d*). Therefore, no adjustment
269 was made for size in the subsequent analyses. Notably, for eight of the characters, including
270 body length, width and haptor length, the polystomatids from southwestern hosts displayed a
271 greater range of measurements than their counterparts from northeastern hosts (Figure 3).

272 Polystomatids from southwestern frog hosts had significantly longer and wider eggs than
273 those from northeastern hosts (Figure 3*e–f*). There were marked differences in the gut
274 morphology between the polystomatids from the two regions. Polystomatids from southwestern
275 frog hosts had significantly more medial and lateral diverticula of the caeca than those from
276 the northeastern hosts (Figure 3*g–h*). On the other hand, even though there were some
277 northeastern polystomatids with up to four post-ovarian intercaecal anastomoses, as opposed
278 to their southwestern counterparts where no specimen had more than two, there was no
279 significant difference in this character between polystomatids from these two regions (Figure
280 3*i*). In terms of large hamulus shape and size, there was no overall difference in the length of
281 the dorsal and ventral roots of the large hamuli between polystomatids from the two regions
282 (Figure 3*j–k*). However, southwestern polystomatids had significantly longer terminal hooks

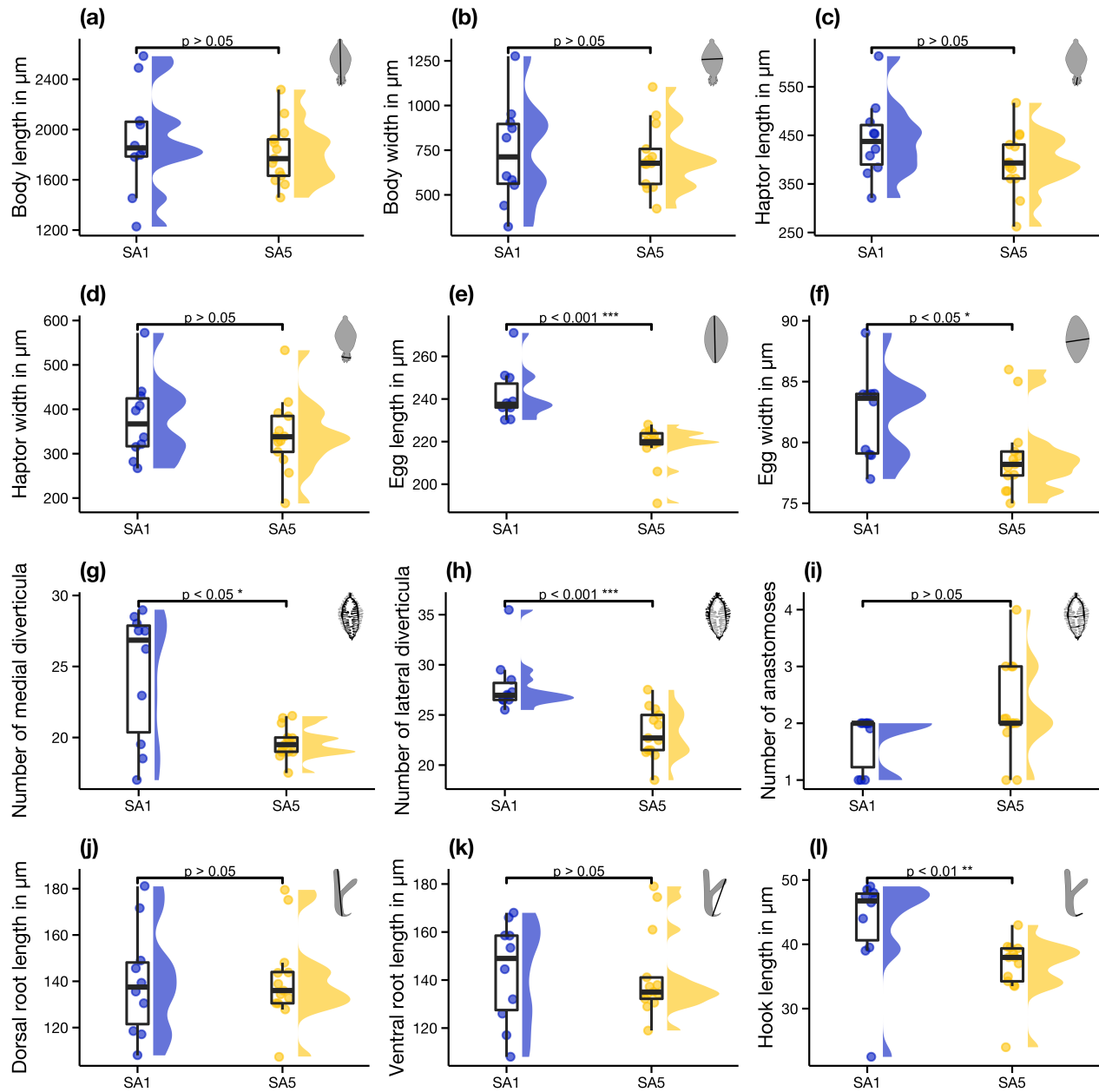


FIGURE 3 Raincloud plots of 12 morphometric characters of the parasite *Protopolystoma xenopodis*, compared based on the geographic origin of their host *Xenopus laevis*, namely SA1 and SA5. The characters are (a) body length, (b) width, (c) haptor length, (d) width, (e) egg length, (f) width, (g) number of medial, (h) lateral diverticula and (i) post-ovarian intercaecal anastomoses, (j) length of the dorsal root, (k) ventral root and (l) terminal hook of the large hamuli. Points indicate raw data along with their distributions to the right and summary statistics, the first, second and third quartiles, are given in boxplots to the left. The brackets above the plots indicate the significance levels calculated by Wilcoxon-Mann-Whitney tests that compared the characters between the two groups.

283 than the northeastern polystomatids (Figure 3/).

284 Thus, *P. xenopodis* from the southwestern region displayed less variation in the number

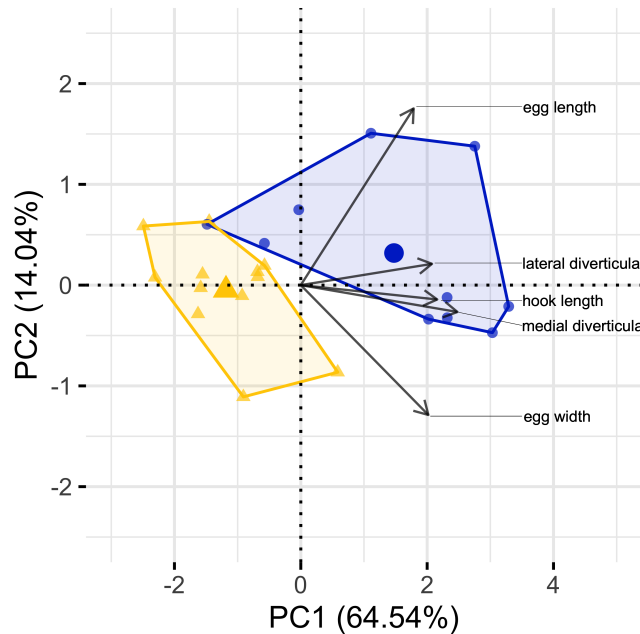


FIGURE 4 The first two principal components derived from five morphometric variables—length and width of the egg, length of the terminal hooks of the hamuli (in μm) and the number of lateral and medial diverticula—of 23 *Protopolystoma xenopodis* associated with the southwestern (SA1, circles in blue) and northeastern (SA5, triangles in yellow) phylogeographic lineages of its frog host *Xenopus laevis*.

285 of anastomoses (SA1_{min:max} = 1–2; SA5_{min:max} = 1–4), possessed more diverticula, both
286 laterally (SA1_{median} = 27; SA5_{median} = 23) and medially (SA1_{median} = 28; SA5_{median} = 20),
287 had longer terminal hooks of the hamuli (SA1_{median} = 46.75 μm ; SA5_{median} = 36.50 μm) and
288 had longer (SA1_{median} = 250.0 μm ; SA5_{median} = 220.5 μm) and wider eggs (SA1_{median} = 84
289 μm ; SA5_{median} = 78 μm) than their northeastern counterparts. Moreover, egg length was a
290 diagnostic character, with no overlap in measurements observed between the two groups of
291 polystomatids (SA1_{min:max} = 236–271 μm ; SA5_{min:max} = 191–228 μm).

292 According to the results of the PCA, the combination of the five significantly different
293 morphological characters, namely egg length and width, terminal hook length and number of
294 lateral and medial diverticula, allowed reasonable discrimination between the polystomatids
295 from the two host lineages (Figure 4). The first two principal components (PCs) accounted for
296 64.54% and 14.04% of the observed variance, together explaining 78.58% of the variance in
297 the data. The loadings of PC1 and PC2 were both positive and negative.

298 3.2 Phylogenetic divergence

299 In the case of the partial *28S rDNA* alignment without the outgroup sequence, a total of 1721
300 bases contained 18 variable and 7 parsimony informative sites. Model-corrected genetic
301 distances in the *28S rDNA* sequences among the six specimens ranged from 0 to 1.6% (Table
302 2). The partial *12S rDNA* data set without the outgroup sequence was represented by an
303 alignment of 505 base pairs. Of the 505 sites, 67 sites were variable and 23 were parsimony
304 informative. Model-corrected genetic distances in the *12S rDNA* sequences among the six
305 *P. xenopodis* specimens ranged from 0.12 to 3.77% (Table 2). For the *COX1* gene alignment,
306 the data set without the outgroup amounted to 418 base pairs, where 25 of the 74 variable
307 sites were parsimony informative. Model-corrected genetic distances in the *COX1* sequences
308 among the six specimens ranged from 0.14 to 9.00% (Table 2). The concatenation of the three
309 alignments with the outgroup sequences, which was used for the subsequent phylogenetic
310 analyses, yielded a total of 2667 base pairs. There were 250 variable sites, of which 93 were
311 parsimony informative.

312 In agreement with the morphometric analyses, phylogenetic tree reconstruction based
313 on the concatenated *12S* and *28S rDNA* and *COX1* gene alignments revealed remarkable
314 divergence in *P. xenopodis* based upon geographic origin. Polystomatids from the SA5 localities
315 formed a well-supported clade (Figure 5). *Protopolystoma xenopodis* from Hermanus and
316 Cape Town (SA1) were earlier diverging than those from the SA5 localities and were rendered
317 paraphyletic by the SA5 lineage in both the BI and ML analyses. Additionally, the BI could not
318 resolve the relationships between *P. xenopodis* from Dullstroom, Tzaneen and Potchefstroom
319 (SA5), even though the sister relationship of *P. xenopodis* from Potchefstroom and Tzaneen to
320 *P. xenopodis* from Dullstroom had high support in the ML.

TABLE 2 Pairwise genetic distances (%) of three partial gene sequences from six specimens of *Protopolystoma xenopodis* from *Xenopus laevis* collected at six localities, here named according to the nearest town. Model-corrected distances are given above the diagonal and percentage of non-identical bases are given below.

	CPT	HRM	MDM	DLS	TZN	PTC
Nuclear 28S rDNA						
Cape Town (CPT)	-	0.05	0.42	0.40	0.50	0.56
Hermanus (HRM)	0.09	-	0.37	0.36	0.61	0.48
Modimolle (MDM)	0.53	0.59	-	0.74	1.60	0.85
Dullstroom (DLS)	0.47	0.53	0.88	-	0.00	0.07
Tzaneen (TZN)	0.47	0.53	0.88	0.00	-	0.05
Potchefstroom (PTS)	0.59	0.65	0.10	0.12	0.06	-
Mitochondrial 12S rDNA						
Cape Town (CPT)	-	2.17	2.02	2.15	2.15	2.11
Hermanus (HRM)	9.76	-	1.39	3.77	1.37	1.37
Modimolle (MDM)	10.18	4.50	-	2.45	0.41	0.40
Dullstroom (DLS)	10.14	6.52	6.94	-	2.87	2.70
Tzaneen (TZN)	9.96	4.08	1.02	6.52	-	0.12
Potchefstroom (PTS)	10.37	4.08	1.02	6.92	0.41	-
Mitochondrial COX1 gene						
Cape Town (CPT)	-	9.00	9.00	9.00	9.00	9.00
Hermanus (HRM)	11.99	-	0.24	9.00	0.29	0.32
Modimolle (MDM)	12.98	4.09	-	9.00	0.20	0.23
Dullstroom (DLS)	12.23	7.43	8.89	-	9.00	9.00
Tzaneen (TZN)	13.19	3.84	2.40	9.11	-	0.14
Potchefstroom (PTS)	12.47	4.32	2.64	8.39	1.68	-

321 4 DISCUSSION

322 The present investigation is the first integrative approach to the intraspecific diversity of
323 *P. xenopodis*, the widespread bladder parasite of the globally invasive frog *X. laevis*. Both mor-
324 phological and molecular data reveal notable intraspecific divergence in *P. xenopodis* collected
325 from two lineages of their host *X. laevis* in South Africa. The combination of egg length and
326 width, number of diverticula of the gut and length of the terminal hook of the large hamulus
327 provides a set of key characters that differentiate northeastern and southwestern populations
328 of *P. xenopodis* in South Africa. Furthermore, the morphological differentiation is supported
329 by the results of the multilocus phylogenetic analyses. Moreover, this intraspecific divergence
330 corresponds to the documented phylogeographic structuring of the host *X. laevis* in its native
331 range (Furman *et al.*, 2015).

Intraspecific divergence in *Protopolystoma xenopodis*

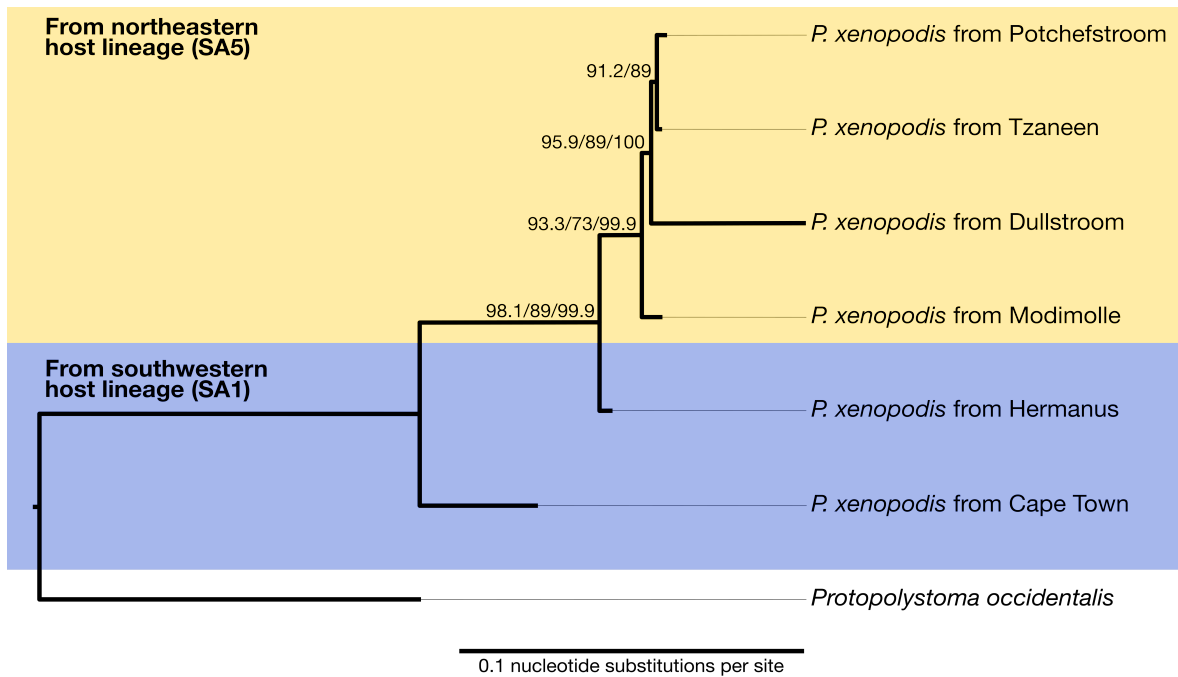


FIGURE 5 Maximum likelihood consensus phylogram of six *Protopolystoma xenopodis* specimens, inferred from the *COX1* gene and *12S* and *28S rDNA* sequences. The polystomatids were recovered at six localities, indicated by the name of the nearest town, from *Xenopus laevis* frog hosts from two phylogeographic lineages (SA1 in blue, SA5 in yellow). The closely related *P. occidentalis* from *X. muelleri* from Togo was used to root the phylogram. Values at the nodes indicate support, where available, as calculated by ultrafast bootstrapping (first value), SH-like approximate likelihood ratio test (second value) and posterior probabilities (third value).

332 Intraspecific variation in morphological characters has been reported before in many species
333 of Polystomatidae and herein *P. xenopodis* is no exception. Especially the number of inter-
334 caecal anastomoses and medial and lateral diverticula are suggested as highly variable
335 characters in polystomatid monogeneans, including *P. xenopodis* (e.g. Aisien & du Preez, 2009;
336 du Preez *et al.*, 2002; Tinsley, 1974, 1978; Tinsley & Jackson, 1998b). Likewise, the high
337 variability in the length of the terminal hook of the large hamulus and genital spine length in
338 *P. xenopodis* has been pointed out previously (Tinsley & Jackson, 1998b). Yet, genital spine
339 length in *P. xenopodis* is the only character for which the link between morphological variation
340 and geographic distance has been explored to date (Tinsley & Jackson, 1998b). Unfortunately,
341 genital spine length could not be measured in the present study. The mounting procedure that
342 we applied to the available specimens, whilst it is ideal for measurements of the soft structures

343 and large hamuli, does not allow for sufficient flattening of the specimens to ensure that the
344 smaller sclerites, such as the genital spines and marginal hooklets, are mounted horizontally.

345 In accordance with the variation in morphometrical characters, the mitochondrial *COX1*
346 gene and *12S rDNA* show remarkable intraspecific divergence both within and between the
347 southwestern and northeastern clusters of *P. xenopodis*. In fact, the divergence in the *COX1*
348 gene of *P. xenopodis* far exceeds that of *Madapolystoma* spec. from frog hosts across Mada-
349 gascar (between 1.7 and 13.2% for *P. xenopodis* and 0.3 and 1.8% in *Madapolystoma* spec.),
350 the only other polystomatid genus for which intraspecific genetic variation has been assessed
351 to date (Berthier *et al.*, 2014). This points towards the nuclear *28S rDNA* as a more useful
352 marker for species recognition in *Protopolystoma*. Yet, even for the *28S rDNA*, intraspecific
353 divergence in *P. xenopodis* is generally higher than what was reported for *Madapolystoma*
354 spec. (between 0.1 and 1.6% for *P. xenopodis* and 0.08 and 0.23% in *Madapolystoma* spec.)
355 (Berthier *et al.*, 2014). The observed geographic variation suggests that future taxonomic
356 studies of Polystomatidae should make use of geographically representative data sets, both
357 when relying on traditional morphometric and advanced molecular approaches.

358 Nonetheless, given the overlap in measurements between the specimens of *P. xenopodis*
359 from different geographic regions, we assume that the observed divergence is still within the
360 bounds of intraspecific variation. It is important to keep in mind that the examined parasites
361 hail from the two most geographically distanced lineages of the host (de Busschere *et al.*,
362 2016; Furman *et al.*, 2015). With the addition of specimens collected from the frog hosts
363 that hail from localities between these two areas, geographically speaking, it is not unrealistic
364 to imagine that morphological variation will present itself on a spectrum that correlates with
365 geographical distance. This is in accordance with the "significant, but continuous" variation in
366 genital spine length that was observed in the study by Tinsley & Jackson (1998b). Likewise,
367 similar investigations of fishes and reptiles revealed that potentially interesting phenotypic
368 divergence was initially reported simply because only the extremes of the distributional range

369 were considered—once the intermediate populations were included in the analyses, phenotypic
370 variation represented geographical variation along a cline (e.g., Ennen *et al.*, 2014; Manier,
371 2004; Risch & Snoeks, 2008; van Steenberge *et al.*, 2011, 2015).

372 On the face of it, one could interpret the observed morphometric variation against the
373 backdrop of the different climatic conditions on either side of the Great Escarpment where our
374 specimens were collected, namely summer rainfall regime to the northeast and a winter rainfall
375 regime to the southwest. Indeed, phenotypic plasticity is a common response to changes in
376 environmental conditions in representatives of Monogenea. This is true of the shape of the
377 hamuli in gyrodactylid species, which has been shown to vary with temperature in isogenic
378 lineages (Olstad *et al.*, 2009). Moreover, both Harris (1998) and Hahn *et al.* (2011) suggested
379 that most of the infrapopulation morphological variation in gyrodactylids can be ascribed to
380 environmental drivers, since it could not be reliably linked to genetic differences. In the case of a
381 capsalid monogenean, temperature differences under experimental conditions drove differences
382 relating to body size, but not relating to the size and shape of sclerotised features (Brazenor
383 *et al.*, 2018). In *P. xenopodis*, temperature can influence egg production rate in the laboratory
384 (Jackson & Tinsley, 1988). Lamentably, the influence of temperature on egg dimensions has
385 not been investigated. All in all, there is evidence that environmental parameters, especially
386 temperature fluctuations, can drive morphological variation in Monogenea within populations or
387 under experimental conditions. However, it is less likely to be the cause of between-population
388 morphological variation, as is revealed by our study.

389 When both the morphological and molecular lines of evidence are considered, it becomes
390 clear that the observed variation in *P. xenopodis* is not merely the product of plasticity during
391 ontogenic development in response to differing climatic conditions. Firstly, the morphological dif-
392 ferentiation between the specimens from the two host lineages involves some of the characters
393 that are important for species delineation in the genus, such as gut and hamulus morphology
394 (Tinsley & Jackson, 1998b). This hints at a link with incipient speciation. Secondly, the observed

395 morphological differences correspond to marked phylogenetic divergence on the intraspecific
396 level in both mitochondrial and nuclear genes of *P. xenopodis*. This divergence echoes the
397 phylogeographic structuring of its frog host across South Africa (Furman *et al.*, 2015), hinting at
398 congruence between the intraspecific diversification of *X. laevis* and *P. xenopodis*, which may
399 be explored in future studies.

400 The Great Escarpment is a well-studied landscape barrier that seems to have shaped the
401 diversification or restricted the expansion of a great many species in South Africa, including
402 representatives of insects, frogs, snakes, lizards and small mammals (e.g. Barlow *et al.*, 2013;
403 Makokha *et al.*, 2007; Mynhardt *et al.*, 2015; Nielsen *et al.*, 2018; Predel *et al.*, 2012). This
404 geological feature likely also had an impact on population structure within the African Clawed
405 Frog *X. laevis* (Furman *et al.*, 2015). Thus, in the light of the high host specificity and ancient
406 association of *Xenopus* and *Protopolystoma* species (Tinsley & Jackson, 1998a), it comes as
407 no surprise that the phylogeographic divergence in *X. laevis* on either side of the Escarpment
408 is mirrored in the morphological, and especially phylogenetic, divergence of *P. xenopodis*.
409 Nonetheless, the Escarpment is no barrier to the well-documented human-mediated domestic
410 translocation of *X. laevis* from the southernmost part of its range to other localities in southern
411 Africa (Measey & Davies, 2011; van Sittert & Measey, 2016). This widespread phenomenon
412 could also contribute to the spread of co-translocated southernmost *P. xenopodis* to the northern
413 parts of its range, which is clearly possible when one considers *P. xenopodis*' co-introduction
414 into the invasive range (Schoeman *et al.*, 2019). As a next step, more detailed investigations
415 that consider the phylogeography of corresponding host-parasite pairs could shed light on
416 the evolutionary and ecological repercussions of the anthropogenic movement of *X. laevis* in
417 southern Africa.

418 In sum, there are clear indications of geographic variation in *P. xenopodis* in South Africa,
419 despite the low sample sizes and patchy geographic presentation of the present study. The
420 findings of this exploratory study open new avenues of investigation for this widespread host-

421 parasite system. Based upon the integration of morphometry and multilocus phylogenetics, our
422 findings bring to light a possible link between the evolutionary histories of both frog host and
423 flatworm parasite. The corresponding morphological and molecular divergence of both *X. laevis*
424 and *P. xenopodis* is a factor to keep in mind in terms of their ability to colonise and adapt to
425 new environments, as was noted for invasive *X. laevis* in France (de Busschere *et al.*, 2016). In
426 addition, the phylogeographic analysis of *P. xenopodis* has the potential to act as a key piece of
427 evidence in the reconstruction of the invasion histories of *X. laevis*, as has been demonstrated
428 in a handful of other studies on the monogenean parasites of invasive fish (Huyse *et al.*, 2015;
429 Kmentová *et al.*, 2019; Ondračková *et al.*, 2012). Ultimately, the newly revealed geographic
430 variation in the most common parasite of *X. laevis* demonstrates that we have barely scratched
431 the surface when it comes to understanding the native parasite dynamics of the world's most
432 widespread amphibian.

433 ACKNOWLEDGEMENTS

434 The authors express their sincere thanks to the farm and smallholding owners who graciously
435 gave permission for collection to take place on their properties and who provided lodging for
436 the research team: Fanus and Olga Kritzinger, Tobie Bielt and Gert Bench. In addition, we
437 thank Mathys Schoeman and Roxanne Viviers who also assisted with fieldwork. The utilisation
438 of the frogs and the research protocols were approved by the Animal Care, Health and Safety
439 in Research Ethics (AnimCare) Committee of the Faculty of Health Sciences of the North-West
440 University (ethics number: NWU-0380-16-A5-01). Animals were sampled under the permit
441 0056-AAA007-00224 (CapeNature) provided by the Department of Economic Development,
442 Environmental Affairs and Tourism. Special Research Funds (BOF) of UHasselt supported
443 MPMV (no. BOF20TT06) and NK (no. BOF21PD01). We further acknowledge the financial
444 support of the National Research Foundation (NRF) of South Africa. ALS received funding from
445 the DSI-NRF Centre of Excellence for Invasion Biology and from the NRF South African Institute

446 for Aquatic Biodiversity. LHdP is indebted to the NRF Foundational Biodiversity Information
447 Programme (no. 120782) for financial support. Any opinion, findings and conclusions or
448 recommendations expressed in this material are those of the authors and the NRF does not
449 accept any liability in this regard.

450 REFERENCES

- 451 Aisien, M. S. O. & du Preez, L. H. 2009. A redescription of *Polystoma africanum* Szidat, 1932
452 (Monogenea: Polystomatidae). *Zootaxa*, 2095:37–46
- 453 Barlow, A., Baker, K., Hendry, C. R., Peppin, L., Phelps, T., Tolley, K. A., ... Wüster, W.
454 2013. Phylogeography of the widespread African puff adder (*Bitis arietans*) reveals multiple
455 Pleistocene refugia in southern Africa. *Molecular Ecology*, 22:1134–1157
- 456 Berthier, P., du Preez, L. H., Raharivololoniana, L., Vences, M. & Verneau, O. 2014. Two new
457 species of polystomes (Monogenea: Polystomatidae) from the anuran host *Guibemantis liber*.
458 *Parasitology International*, 63:108–119. <https://doi.org/10.1016/j.parint.2013.09.014>
- 459 Blackburn, T. M. & Ewen, J. G. 2017. Parasites as drivers and passengers of human-mediated
460 biological invasions. *EcoHealth*, 14:61–73. <https://doi.org/10.1007/s10393-015-1092-6>
- 461 Brazenor, A. K., Saunders, R. J., Miller, T. L. & Hutson, K. S. 2018. Morphological variation in the
462 cosmopolitan fish parasite *Neobenedenia girellae* (Capsalidae: Monogenea). *International*
463 *Journal for Parasitology*, 48:125–134
- 464 Chernomor, O., von Haeseler, A. & Minh, B. Q. 2016. Terrace aware data structure for
465 phylogenomic inference from supermatrices. *Systematic Biology*, 65:997–1008. <https://doi.org/10.1093/sysbio/syw037>
- 467 Constantin, A.-E. & Patil, I. 2021. ggsignif: R package for displaying significance brackets for
468 'ggplot2'. *PsyArxiv*. <https://doi.org/10.31234/osf.io/7awm6>
- 469 de Busschere, C., Courant, J., Herrel, A., Rebelo, R., Rödder, D., Measey, G. J. & Backeljau,
470 T. 2016. Unequal contribution of native South African phylogeographic lineages to the

- 471 invasion of the African clawed frog, *Xenopus laevis*, in Europe. *PeerJ*, 4, e1659. <https://doi.org/10.7717/peerj.1659>
- 472
- 473 du Preez, L. H., Kunene, N., Hanner, R., Giesy, J. P., Solomon, K. R., Hosmer, A. & van der
- 474 Kraak, G. J. 2009. Population-specific incidence of testicular ovarian follicles in *Xenopus*
- 475 *laevis* from South Africa: a potential issue in endocrine testing. *Aquatic Toxicology*, 95:10–16.
- 476 <https://doi.org/10.1016/j.aquatox.2009.07.018>
- 477 du Preez, L. H., Vaucher, C. & Mariaux, J. 2002. Polystomatidae (Monogenea) of African
- 478 Anura: *Polystoma dawiekoki* n. sp. parasitic in *Ptychadena anchietae* (Bocage). *Systematic*
- 479 *Parasitology*, 52:35–41
- 480 Edgar, R. C. 2004. MUSCLE: multiple sequence alignment with high accuracy and high
- 481 throughput. *Nucleic Acids Research*, 32:1792–1797. <https://doi.org/10.1093/nar/gkh340>
- 482 Ennen, J. R., Kalis, M. E., Patterson, A. L., Kreiser, B. R., Lovich, J. E., Godwin, J. & Qualls, C. P.
- 483 2014. Clinal variation or validation of a subspecies? A case study of the *Graptemys nigrinoda*
- 484 complex (Testudines: Emydidae). *Biological Journal of the Linnean Society*, 111:810–822.
- 485 <https://doi.org/10.1111/bij.12234>
- 486 Furman, B. L., Bewick, A. J., Harrison, T. L., Greenbaum, E., Gvozdik, V., Kusamba, C. &
- 487 Evans, B. J. 2015. Pan-African phylogeography of a model organism, the African clawed frog
- 488 *Xenopus laevis*. *Molecular Ecology*, 24:909–925. <https://doi.org/10.1111/mec.13076>
- 489 Gouy, M., Guindon, S. & Gascuel, O. 2010. SeaView version 4: a multiplatform graphical
- 490 user interface for sequence alignment and phylogenetic tree building. *Molecular Biology and*
- 491 *Evolution*, 27:221–224. <https://doi.org/10.1093/molbev/msp259>
- 492 Grohovaz, G. S., Harley, E. & Fabian, B. 1996. Significant mitochondrial DNA sequence diver-
- 493 gence in natural populations of *Xenopus laevis* (Pipidae) from South Africa. *Herpetologica*,
- 494 52:247–253. <https://doi.org/10.1080/11250003.2013.847502>
- 495 Gu, X., Fu, Y. X. & Li, W. H. 1995. Maximum likelihood estimation of the heterogeneity of
- 496 substitution rate among nucleotide sites. *Molecular Biology and Evolution*, 12:546–557.

- 497 <https://doi.org/10.1093/oxfordjournals.molbev.a040235>
- 498 Guindon, S., Dufayard, J. F., Lefort, V., Anisimova, M., Hordijk, W. & Gascuel, O. 2010.
499 New algorithms and methods to estimate maximum-likelihood phylogenies: assessing the
500 performance of PhyML 3.0. *Systematic Biology*, 59:307–321. [https://doi.org/10.1093/sysbio/](https://doi.org/10.1093/sysbio/syq010)
501 [syq010](https://doi.org/10.1093/sysbio/syq010)
- 502 Hahn, C., Bakke, T. A., Bachmann, L., Weiss, S. & Harris, P. D. 2011. Morphometric and molec-
503 ular characterization of *Gyrodactylus teuchis* Lutraite, Blanc, Thiery, Daniel & Vigneulle,
504 1999 (Monogenea: Gyrodactylidae) from an Austrian brown trout population. *Parasitology*
505 *International*, 60:480–487. <https://doi.org/10.1016/j.parint.2011.08.016>
- 506 Harris, P. D. 1998. Ecological and genetic evidence for clonal reproduction in *Gyrodactylus*
507 *gasterostei* Glaser, 1974. *International Journal for Parasitology*, 28:1595–1607
- 508 Hasegawa, M., Kishino, H. & Yano, T. 1985. Dating of the human-ape splitting by a molecular
509 clock of mitochondrial DNA. *Journal of Molecular Evolution*, 22:160–174. [https://doi.org/10.](https://doi.org/10.1007/BF02101694)
510 [1007/BF02101694](https://doi.org/10.1007/BF02101694)
- 511 Héritier, L., Badets, M., du Preez, L. H., Aisien, M. S., Lixian, F., Combes, C. & Verneau, O. 2015.
512 Evolutionary processes involved in the diversification of chelonian and mammal polystomatid
513 parasites (Platyhelminthes, Monogenea, Polystomatidae) revealed by palaeoecology of their
514 hosts. *Molecular Phylogenetics and Evolution*, 92:1–10. [https://doi.org/10.1016/j.ympev.2015.](https://doi.org/10.1016/j.ympev.2015.05.026)
515 [05.026](https://doi.org/10.1016/j.ympev.2015.05.026)
- 516 Héritier, L., Verneau, O., Smith, K. G., Coetzer, C. & du Preez, L. H. 2018. Demonstrating the
517 value and importance of combining DNA barcodes and discriminant morphological characters
518 for polystome taxonomy (Platyhelminthes, Monogenea). *Parasitology International*, 67:38–46.
519 <https://doi.org/10.1016/j.parint.2017.03.002>
- 520 Hoang, D. T., Chernomor, O., von Haeseler, A., Minh, B. Q. & Vinh, L. S. 2018. UFBoot2:
521 improving the ultrafast bootstrap approximation. *Molecular Biology and Evolution*, 35:518–
522 522. <https://doi.org/10.1093/molbev/msx281>

- 523 Huysel, T., Vanhove, M. P. M., Mombaerts, M., Volckaert, F. A. M. & Verreycken, H. 2015.
524 Parasite introduction with an invasive goby in Belgium: double trouble? *Parasitology*
525 *Research*, 114:2789–2793. <https://doi.org/10.1007/s00436-015-4544-6>
- 526 Jackson, H. C. & Tinsley, R. C. 1988. Environmental influences on egg production by the
527 monogenean *Protopolystoma xenopodis*. *Parasitology*, 97:115–128. [https://doi.org/10.1017/](https://doi.org/10.1017/S0031182000066798)
528 S0031182000066798
- 529 Kalyaanamoorthy, S., Minh, B. Q., Wong, T. K. F., von Haeseler, A. & Jermiin, L. S. 2017.
530 ModelFinder: fast model selection for accurate phylogenetic estimates. *Nature Methods*,
531 14:587–589. <https://doi.org/10.1038/nmeth.4285>
- 532 Kassambara, A. & Mundt, F. 2020. *factoextra: extract and visualize the results of multivariate*
533 *data analyses. R package version 1.0.7.*
- 534 Kay, M. 2021. ggdist: Visualizations of Distributions and Uncertainty. R package *version 3.0.1.*
535 <https://doi.org/10.5281/zenodo.3879620>
- 536 Kimura, M. 1981. Estimation of evolutionary distances between homologous nucleotide se-
537 quences. *Proceedings of the National Academy of Sciences USA*, 78:454–458. <https://doi.org/10.1073/pnas.78.1.454>
- 538
- 539 Kmentová, N., van Steenberge, M., van den Audenaerde, D. F. E. T., Nhiwatiwa, T.,
540 Muterezi Bukinga, F., Mulimbwa N'Sibula, T., ... Vanhove, M. P. M. 2019. Co-introduction
541 success of monogeneans infecting the fisheries target *Limnothrissa miodon* differs between
542 two non-native areas: the potential of parasites as a tag for introduction pathway. *Biological*
543 *Invasions*, 21:757–773. <https://doi.org/10.1007/s10530-018-1856-3>
- 544 Kuperman, B. I., Matey, V. E., Fisher, R. N., Ervin, E. L., Warburton, M. L., Bakhireva, L. &
545 Lehman, C. A. 2004. Parasites of the African Clawed Frog, *Xenopus laevis*, in Southern
546 California, U.S.A. *Comparative Parasitology*, 71:229–232. <https://doi.org/10.1654/4112>
- 547 Lee, C. E. & Gelembiuk, G. W. 2008. Evolutionary origins of invasive populations. *Evolutionary*
548 *Applications*, 1:427–448. <https://doi.org/10.1111/j.1752-4571.2008.00039.x>

- 549 Lin Pedersen, T. 2020. patchwork: the composer of plots. R package version 1.1.1. <https://doi.org/https://CRAN.R-project.org/package=patchwork>
- 550
- 551 Littlewood, D. T. J., Rohde, K. & Clough, K. A. 1997. Parasite speciation within or between host
552 species? – Phylogenetic evidence from site-specific polystome monogeneans. *International*
553 *Journal for Parasitology*, 27:1289–1297. [https://doi.org/10.1016/S0020-7519\(97\)00086-6](https://doi.org/10.1016/S0020-7519(97)00086-6)
- 554 Makokha, J. S., Bauer, A. M., Mayer, W. & Matthee, C. A. 2007. Nuclear and mtDNA-based
555 phylogeny of southern African sand lizards, *Pedioplanis* (Sauria: Lacertidae). *Molecular*
556 *Phylogenetics and Evolution*, 44:622–633
- 557 Manier, M. K. 2004. Geographic variation in the long-nosed snake, *Rhinocheilus lecontei*
558 (Colubridae): beyond the subspecies debate. *Biological Journal of the Linnean Society*,
559 83(1):65–85. <https://doi.org/10.1111/j.1095-8312.2004.00373.x>
- 560 Mazzamuto, M. V., Galimberti, A., Cremonesi, G., Pisanu, B., Chapuis, J.-L., Stuyck, J., ...
561 Martinoli, A. 2016. Preventing species invasion: a role for integrative taxonomy? *Integrative*
562 *Zoology*, 11:214–228. <https://doi.org/10.1111/1749-4877.12185>
- 563 Measey, G. J. & Channing, A. 2003. Phylogeography of the genus *Xenopus* in southern Africa.
564 *Amphibia-Reptilia*, 24:321–330. <https://doi.org/10.1163/156853803322440781>
- 565 Measey, G. J. & Davies, S. J. 2011. Struggling against domestic exotics at the southern end of
566 Africa. *Froglog*, 97:28–30
- 567 Measey, G. J., Rödder, D., Green, S. L., Kobayashi, R., Lillo, F., Lobos, G., ... Thirion, J. M. 2012.
568 Ongoing invasions of the African clawed frog, *Xenopus laevis*: a global review. *Biological*
569 *Invasions*, 14:2255–2270. <https://doi.org/10.1007/s10530-012-0227-8>
- 570 Miller, M. A., Pfeiffer, W. & Schwartz, T. 2010. Creating the CIPRES Science Gateway for
571 inference of large phylogenetic trees. *Conference proceedings. 2010 Gateway Computing*
572 *Environments Workshop (GCE)*: Institute of Electrical and Electronics Engineers.
- 573 Minh, B. Q., Schmidt, H. A., Chernomor, O., Schrempf, D., Woodhams, M. D., von Haeseler A. &
574 Lanfear, R. 2020. IQ-TREE 2: new models and efficient methods for phylogenetic inference

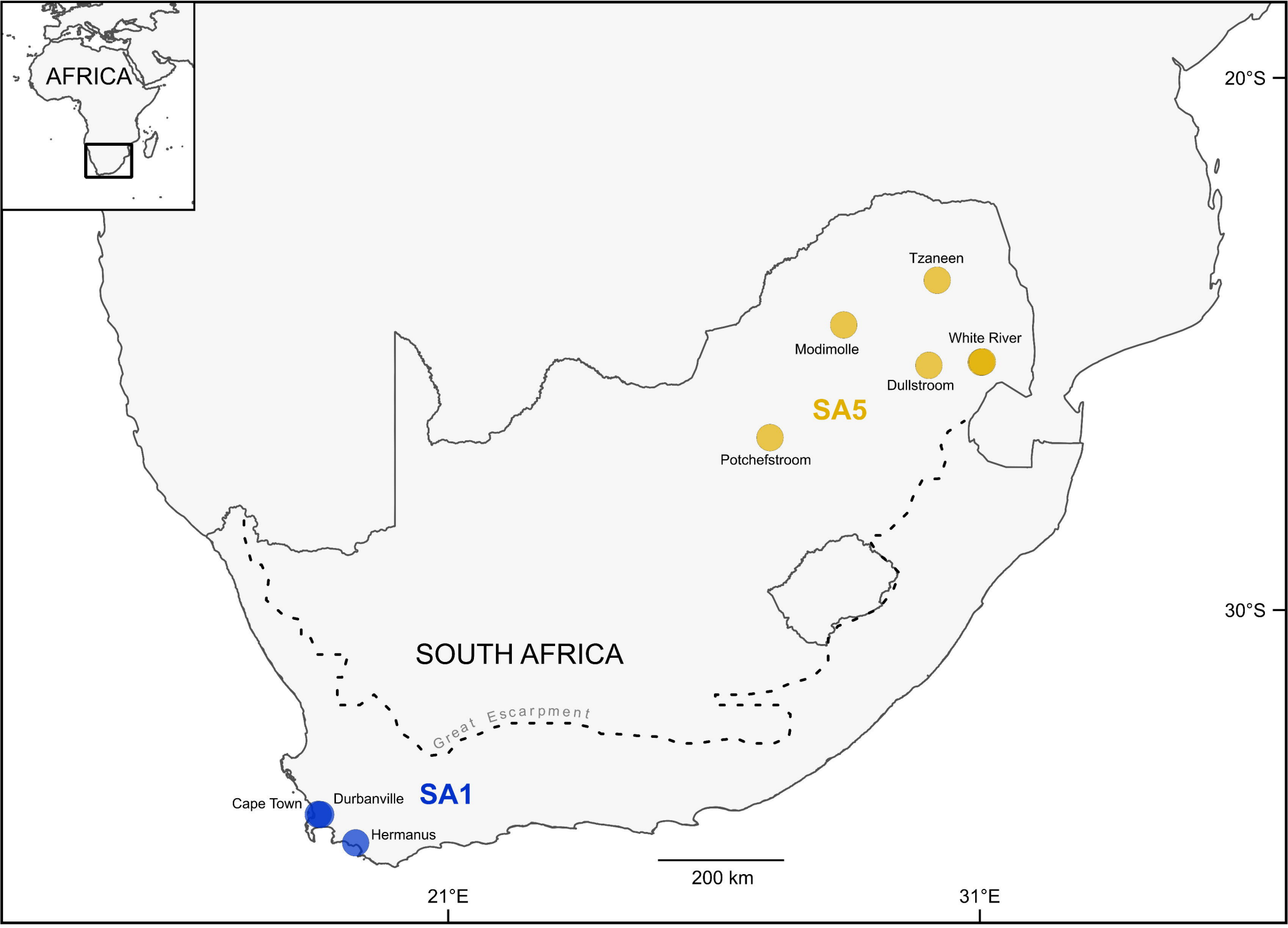
- 575 in the genomic era. *Molecular Biology and Evolution*, 37:1530–1534. [https://doi.org/10.1093/](https://doi.org/10.1093/molbev/msaa015)
576 [molbev/msaa015](https://doi.org/10.1093/molbev/msaa015)
- 577 Mynhardt, S., Maree, S., Pelsler, I., Bennett, N. C., Bronner, G. N., Wilson, J. W. & Bloomer, P.
578 2015. Phylogeography of a morphologically cryptic golden mole assemblage from South-
579 Eastern Africa. *PLOS ONE*, 10, e0144995
- 580 Nguyen, L.-T., Schmidt, H. A., von Haeseler, A. & Minh, B. Q. 2015. IQ-TREE: a fast and
581 effective stochastic algorithm for estimating maximum-likelihood phylogenies. *Molecular*
582 *Biology and Evolution*, 32:268–274. <https://doi.org/10.1093/molbev/msu300>
- 583 Nieberding, C., Morand, S., Libois, R. & Michaux, J. R. 2004. A parasite reveals cryptic
584 phylogeographic history of its host. *Proceedings of the Royal Society B: Biological Sciences*,
585 271:2559–2568. <https://doi.org/10.1098/rspb.2004.2930>
- 586 Nieberding, C. M. & Olivieri, I. 2007. Parasites: proxies for host genealogy and ecology? *Trends*
587 *in Ecology and Evolution*, 22:156–165. <https://doi.org/10.1016/j.tree.2006.11.012>
- 588 Nielsen, S. V., Daniels, S. R., Conradie, W., Heinicke, M. P. & Noonan, B. P. 2018. Multilocus
589 phylogenetics in a widespread African anuran lineage (Brevicipitidae: *Breviceps*) reveals
590 patterns of diversity reflecting geoclimatic change. *Journal of Biogeography*, 45:2067–2079
- 591 Oksanen, J., Blanchet, F. G., Friendly, M., Kindt, R., Legendre, P., McGlinn, D., ... Wagner, H.
592 2020. vegan: community ecology package. R package *version 2.5-7*. [https://doi.org/https://](https://doi.org/https://CRAN.R-project.org/package=vegan)
593 CRAN.R-project.org/package=vegan
- 594 Olstad, K., Bachmann, L. & Bakke, T. 2009. Phenotypic plasticity of taxonomic and diagnostic
595 structures in gyrodactylosis-causing flatworms (Monogenea, Platyhelminthes). *Parasitology*,
596 136:1305–1315
- 597 Ondračková, M., Matějusková, I. & Grabowska, J. 2012. Introduction of *Gyrodactylus perccotti*
598 (Monogenea) into Europe on its invasive fish host, Amur sleeper (*Perccottus glenii*, Dybowski
599 1877). *Helminthologia*, 49:21–26. <https://doi.org/10.2478/s11687-012-0004-3>
- 600 Posada, D. 2003. Using MODELTEST and PAUP* to select a model of nucleotide substitution.

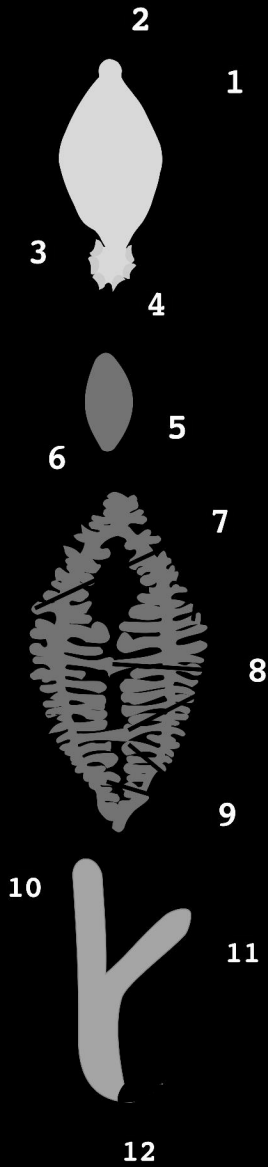
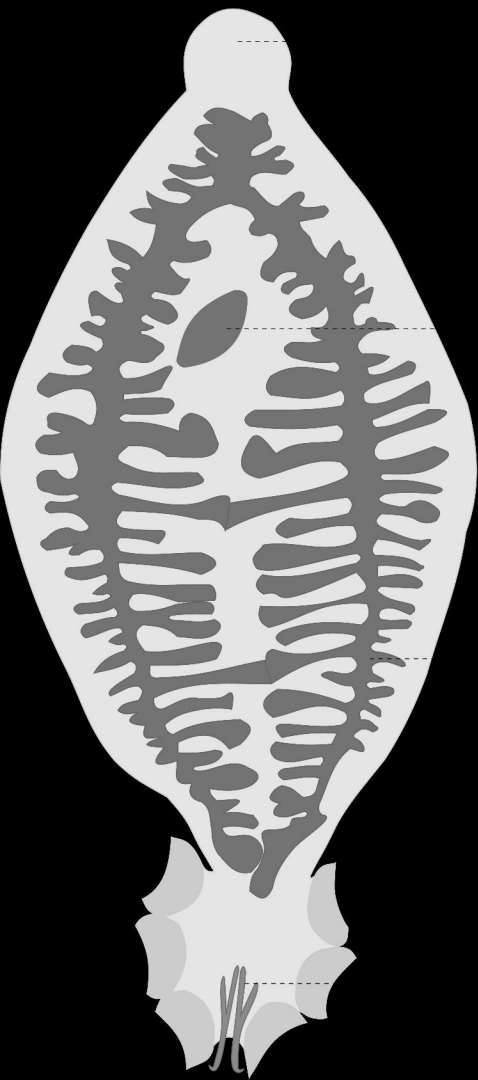
- 601 *Current Protocols in Bioinformatics*, 00:6.5.1–6.5.14. <https://doi.org/10.1002/0471250953>.
- 602 bi0605s00
- 603 Predel, R., Neupert, S., Huetteroth, W., Kahnt, J., Waidelich, D. & Roth, S. 2012. Peptidomics-
604 based phylogeny and biogeography of Mantophasmatodea (Hexapoda). *Systematic Biology*,
605 61:609–629
- 606 QGIS Development Team. 2018. *QGIS Geographic Information System*. Oregon, United States
607 of America: Open Source Geospatial Foundation Project. <http://qgis.osgeo.org/>
- 608 R Core Team. 2021. *R: a language and environment for statistical computing*. Vienna, Austria:
609 R Foundation for Statistical Computing. <https://www.R-project.org/>
- 610 Risch, S. & Snoeks, J. 2008. Geographic variation in *Neolamprologus niger* (Poll, 1956)
611 (Perciformes: Cichlidae) from Lake Tanganyika (Africa). *Zootaxa*, 1857:21–32. [https://doi.](https://doi.org/10.11646/zootaxa.1857.1.2)
612 [org/10.11646/zootaxa.1857.1.2](https://doi.org/10.11646/zootaxa.1857.1.2)
- 613 Robinson, D., Hayes, A. & Couch, S. 2022. broom: convert statistical objects into tidy tibbles. R
614 package version 0.7.11. <https://doi.org/https://CRAN.R-project.org/package=broom>
- 615 Rodrigues, R. A. E. 2014. *Macroparasites of invasive Xenopus laevis (Amphibia: Anura):*
616 *characterization and assessment of possible exchanges with native Pelophylax perezi in*
617 *Oeiras streams, Portugal*. Lisbon: University of Lisboa. (Dissertation – MSc).
- 618 Ronquist, F., Teslenko, M., van der Mark, P., Ayres, D. L., Darling, A., Höhna, S., ... Huelsenbeck,
619 J. P. 2012. MrBayes 3.2: efficient Bayesian phylogenetic inference and model choice across
620 a large model space. *Systematic Biology*, 61:539–542. <https://doi.org/10.1093/sysbio/sys029>
- 621 Schoeman, A. L., Kruger, N., Secondi, J. & du Preez, L. H. 2019. Repeated reduction in
622 parasite diversity in invasive populations of *Xenopus laevis*: a global experiment in enemy
623 release. *Biological Invasions*, 21:1323–1338. <https://doi.org/10.1007/s10530-018-1902-1>
- 624 Snyder, S. D. & Clopton, R. E. 2005. New methods for the collection and preservation of
625 spirorchiid trematodes and polystomatid monogeneans from turtles. *Comparative Parasitol-*
626 *ogy*, 72:102–107. <https://doi.org/10.1654/4155>

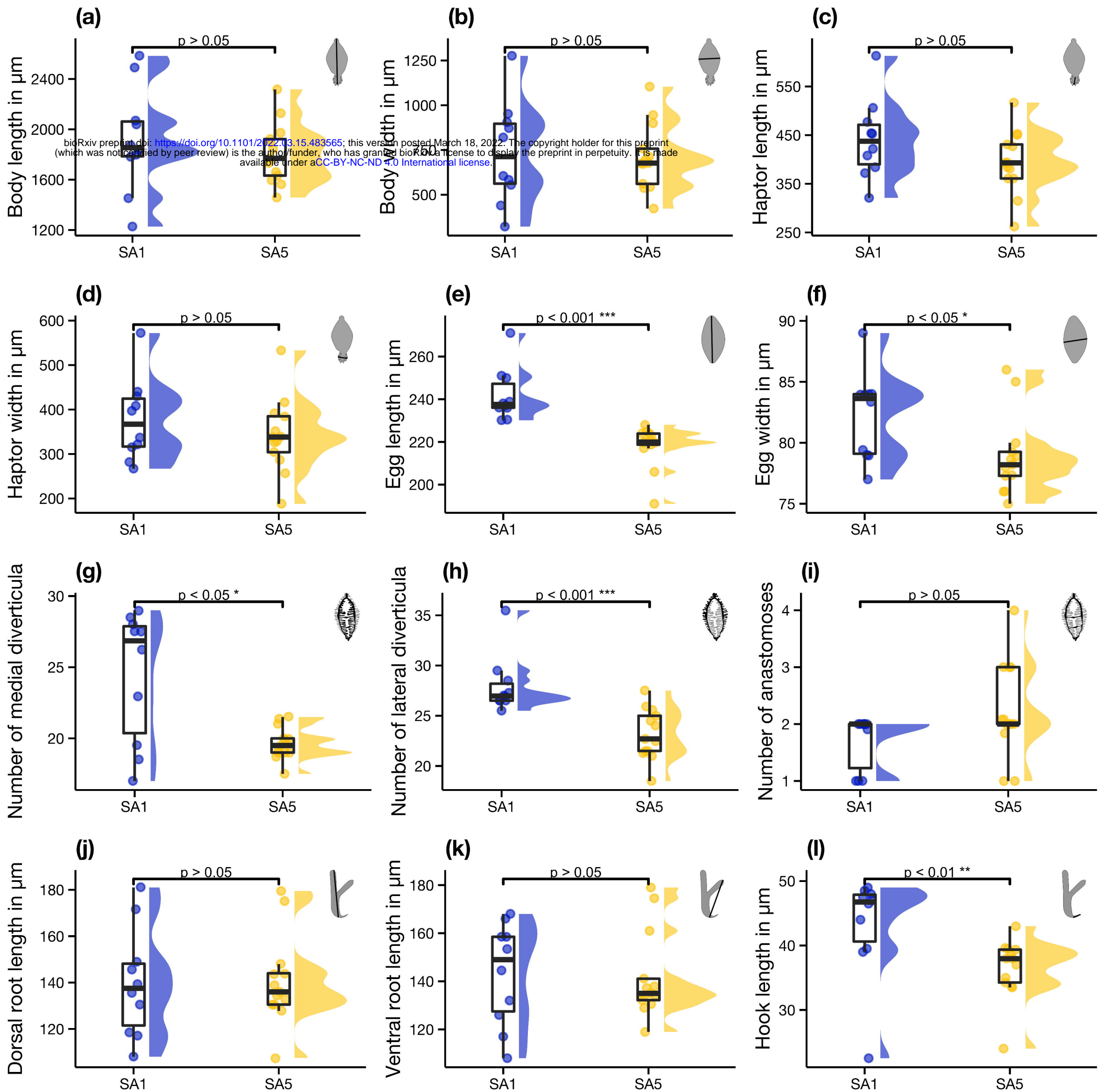
- 627 Soubrier, J., Steel, M., Lee, M. S., Der Sarkissian, C., Guindon, S., Ho, S. Y. & Cooper, A. 2012.
628 The influence of rate heterogeneity among sites on the time dependence of molecular rates.
629 *Molecular Biology and Evolution*, 29:3345–3358. <https://doi.org/10.1093/molbev/mss140>
- 630 Stekhoven, D. J. 2013. missForest: nonparametric missing value imputation using random
631 forest. R package *version 1.4*
- 632 Stekhoven, D. J. & Bühlmann, P. 2012. MissForest: non-parametric missing value imputation for
633 mixed-type data. *Bioinformatics*, 28:112–118. <https://doi.org/10.1093/bioinformatics/btr597>
- 634 Tavaré, S. 1986. Some probabilistic and statistical problems in the analysis of DNA sequences.
635 *Lectures on Mathematics in the Life Sciences*, 17:56–86
- 636 Thorpe, R. S. 1981. A comparative study of ordination techniques in numerical taxonomy in
637 relation to racial variation in the ringed snake *Natrix natrix* (L.). *Biological Journal of the*
638 *Linnean Society*, 13:7–40. <https://doi.org/10.1111/j.1095-8312.1980.tb00067.x>
- 639 Tinsley, R. C. 1974. Observations on *Polystoma africanum* Szidat with a review of the inter-
640 relationships of *Polystoma* species in Africa. *Journal of Natural History*, 8:355–367. <https://doi.org/10.1080/00222937400770311>
- 641
- 642 Tinsley, R. C. 1978. The morphology and distribution of *Eupolystoma* species (Monogenoidea)
643 in Africa, with a description of *E. anterorchis* sp. n. from *Bufo pardalis* at the Cape. *Journal*
644 *of Helminthology*, 52:291–302
- 645 Tinsley, R. C. 1996. Parasites of *Xenopus*. In: Tinsley, R. C. & Kobel, H. R., eds. Vol. 1, *The*
646 *Biology of Xenopus*. Oxford: Clarendon Press. pp. 233–261.
- 647 Tinsley, R. C. & Jackson, J. A. 1998a. Correlation of parasite speciation and specificity
648 with host evolutionary relationships. *International Journal for Parasitology*, 28:1573–1582.
649 [https://doi.org/10.1016/s0020-7519\(98\)00085-x](https://doi.org/10.1016/s0020-7519(98)00085-x)
- 650 Tinsley, R. C. & Jackson, J. A. 1998b. Speciation of *Protopolystoma* Bychowsky, 1957 (Mono-
651 genea: Polystomatidae) in hosts of the genus *Xenopus* (Anura: Pipidae). *Systematic*
652 *Parasitology*, 40:93–141. <https://doi.org/10.1023/B:SYPA.0000004047.41228.a6>

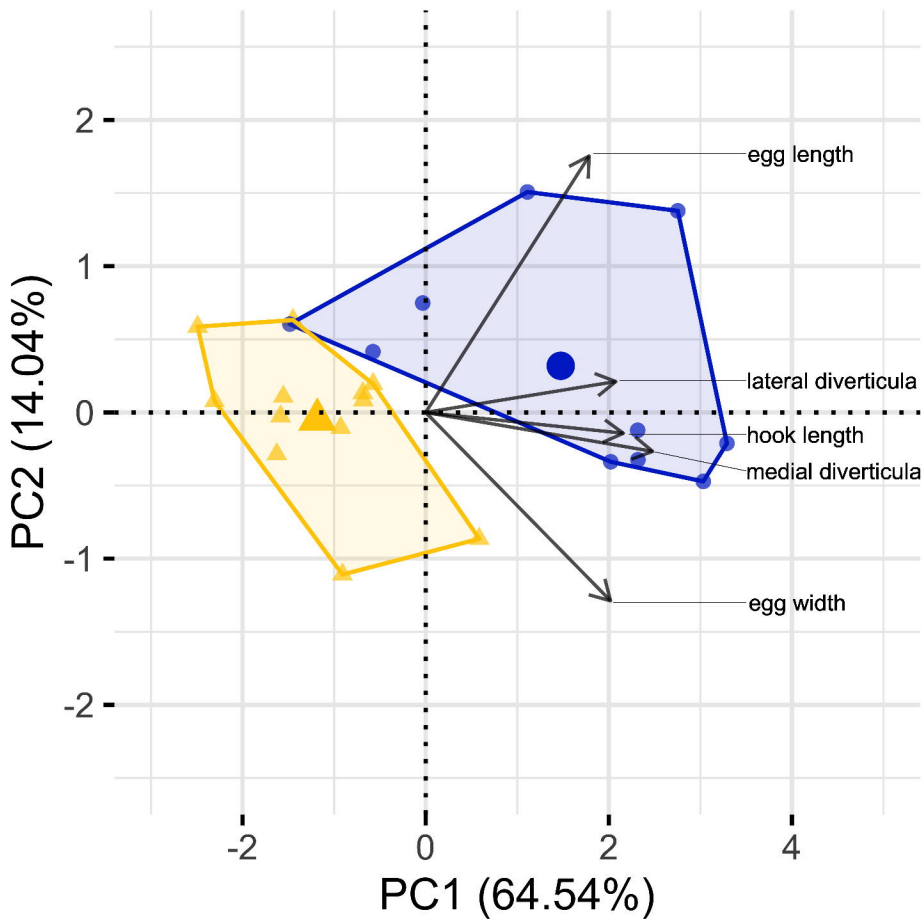
- 653 Tkach, V., Grabda-Kazubska, B., Pawlowski, J. & Swiderski, Z. 1999. Molecular and mor-
654 phological evidence for close phylogenetic affinities of the genera *Macrodera*, *Leptophallus*,
655 *Metaleptophallus* and *Paralepoderma* (Digenea, Plagiorchiata). *Acta Parasitologica*, 44:170–
656 179
- 657 Torchin, M. E., Lafferty, K. D., Dobson, A. P., McKenzie, V. J. & Kuris, A. M. 2003. Intro-
658 duced species and their missing parasites. *Nature*, 421:628–630. [https://doi.org/10.1038/](https://doi.org/10.1038/nature01346)
659 [nature01346](https://doi.org/10.1038/nature01346)
- 660 Trifinopoulos, J., Nguyen, L.-T., von Haeseler, A. & Minh, B. Q. 2016. W-IQ-TREE: a fast online
661 phylogenetic tool for maximum likelihood analysis. *Nucleic Acids Research*, 44:W232–W235.
662 <https://doi.org/10.1093/nar/gkw256>
- 663 Urbanek, S. 2013. png: read and write PNG images. R package version 0.1-7. [https://doi.org/](https://doi.org/https://CRAN.R-project.org/package=png)
664 <https://CRAN.R-project.org/package=png>
- 665 Vaidya, G., Lohman, D. J. & Meier, R. 2011. SequenceMatrix: concatenation software for the
666 fast assembly of multi-gene datasets with character set and codon information. *Cladistics*,
667 27:171–180. <https://doi.org/10.1111/j.1096-0031.2010.00329.x>
- 668 van Sittert, L. & Measey, G. J. 2016. Historical perspectives on global exports and research of
669 African clawed frogs (*Xenopus laevis*). *Transactions of the Royal Society of South Africa*,
670 71:157–166. <https://doi.org/10.1080/0035919x.2016.1158747>
- 671 van Steenberge, M., Pariselle, A., Huyse, T., Volckaert, F. A. M., Snoeks, J. & Vanhove, M. P. M.
672 2015. Morphology, molecules, and monogenean parasites: an example of an integrative
673 approach to cichlid biodiversity. *PLOS ONE*, 10(4):e0124474. [https://doi.org/10.1371/journal.](https://doi.org/10.1371/journal.pone.0124474)
674 [pone.0124474](https://doi.org/10.1371/journal.pone.0124474)
- 675 van Steenberge, M., Vanhove, M. P., Muzumani Riasa, D., Mulimbwa N'Sibula, T.,
676 Muterezi Bukinga, F., Pariselle, A., ... Snoeks, J. 2011. A recent inventory of the fishes of the
677 north-western and central western coast of Lake Tanganyika (Democratic Republic Congo).
678 *Acta Ichthyologica et Piscatoria*, 41(3):201–214. <https://doi.org/10.3750/AIP2011.41.3.08>

- 679 Verneau, O., du Preez, L. H., Laurent, V., Raharivololoniaina, L., Glaw, F. & Vences, M. 2009.
680 The double odyssey of Madagascan polystome flatworms leads to new insights on the
681 origins of their amphibian hosts. *Proceedings of the Royal Society B: Biological Sciences*,
682 276:1575–1583. <https://doi.org/10.1098/rspb.2008.1530>
- 683 Waring, E., Quinn, M., McNamara, A., Arino de la Rubia, E., Zhu, H. & Ellis, S. 2021. skimr:
684 compact and flexible summaries of data. R package *version* 2.1.3. [https://doi.org/https://](https://doi.org/https://CRAN.R-project.org/package=skimr)
685 CRAN.R-project.org/package=skimr
- 686 Wellband, K. W., Pettitt-Wade, H., Fisk, A. T. & Heath, D. D. 2017. Differential invasion
687 success in aquatic invasive species: the role of within-and among-population genetic diversity.
688 *Biological Invasions*, 19:2609–2621. <https://doi.org/10.1007/s10530-017-1471-8>
- 689 Wickham, H., Averick, M., Bryan, J., Chang, W., D'Agostino McGowan, L., François, R., ...
690 Yutani, H. 2019. Welcome to the tidyverse. *Journal of Open Source Software*, 4, art. 1686.
691 <https://doi.org/10.21105/joss.01686>
- 692 Wilke, C. O. 2020. ggtext: improved text rendering support for 'ggplot2'. R package *version*
693 0.1.1. <https://doi.org/https://CRAN.R-project.org/package=ggtext>
- 694 Yang, Z. 1994. Maximum likelihood phylogenetic estimation from DNA sequences with variable
695 rates over sites: approximate methods. *Journal of Molecular Evolution*, 39:306–314. [https://](https://doi.org/10.1007/BF00160154)
696 doi.org/10.1007/BF00160154









**From northeastern
host lineage (SA5)**

91.2/89

P. xenopodis from Potchefstroom

95.9/89/100

P. xenopodis from Tzaneen

93.3/73/99.9

P. xenopodis from Dullstroom

98.1/89/99.9

P. xenopodis from Modimolle

**From southwestern
host lineage (SA1)**

P. xenopodis from Hermanus

P. xenopodis from Cape Town

